ACTIVE CONTROL STICK DRIVEN BY A PIEZO ELECTRIC MOTOR

T. Schulte[1], H. Grotstollen[1], H.-P. Schöner[2], J.-T. Audren[3]

[1]University of Paderborn, Institute of Power Electronics and Electrical Drives, FB14/LEA,
  Warburger Straße 100, D-33098 Paderborn, Germany, Phone ++49-5251-60-3653
[2]DaimlerChrysler, Research and Technology FT2/LA,
  Goldsteinstraße 235, D-60528 Frankfurt, Germany, Phone ++49-69-6679-578
[3]SFIM Industries, Design and Development,
  13, avenue Marcel Ramolfo Garnier, F-91344 Massy Cedex, France, Phone ++33-169-196-721

Abstract – An Active Control Stick (ACS) realized by a travelling wave type ultrasonic motor (USM) is presented. In contrast to the conventional side stick in modern aircrafts, which is only operated by a passive mechanic feedback, forces can be reproduced artificially by an active control stick. Ultrasonic motors are more compact as conventional electrical geared motors and combine features such as high driving torque at low rotational speed and low noise in operation and low electromagnetic emission. In this paper a control schemes for an active control stick using a rotary travelling wave type USM is presented which is already implemented and successfully tested for an one axis prototype version of an ACS within a cooperative project of the Department Research and Technology of the DaimlerChrysler AG in Frankfurt, SFIM Industries and the Institute of Power Electronics and Electrical Drive of the University of Paderborn.

Keywords : Control of Drive Systems, Vibration Control, Mechatronic Systems, Piezomotors.

1. INTRODUCTION

In modern aircrafts like the AIRBUS-series the control stick is realized by a small side stick mounted beside the pilot's seat, where the electrical signals transferred by the stick's electronic are used for controlling the rudders - Fly by Wire. The conventional side stick is only operated by passive mechanics forcing the stick back to its neutral position. The main disadvantage is the absence of any feedback from the rudders.

In order to realize an active control stick an actuator has to be introduced in the mechanical assembly of the stick. The actuator on the one hand generates feedback forces which help the pilot to get a better control on the aircraft and on the other hand it serves for reproducing a nonlinear spring characteristic which otherwise is generated by the passive mechanic of the stick but now can be varied on-line. Additionally the generation of mechanical warning signals in form of stick vibrations and the coupling of pilot's and copilot's sticks are possible when using an ACS.

The mechanical assemblies of previous realizations by use of conventional electrical actuators are huge and heavy. Rotary travelling wave type USMs are more compact as conventional electrical geared motors and have high driving torque at low rotational speed. Due to their low noise in operation and low electromagnetic emission they are suitable for use in aviation. Thus a USM is used here for realizing an one axis active control stick. The motor which is used is the AWM90 (Prototype USM of Daimler-Chrysler) which at the authors best knowledge is presently the most powerful piezo drive.

The driving principle of travelling wave type USMs is based on two orthogonal mechanical vibration modes which are excited in the stator to their single eigenfrequency by a piezo ceramic layer, [1], [2]. Superimposing both standing waves by proper amplitudes and temporal phase shift a travelling bending wave is generated, which performs elliptic motions of the stator's surface points. The rotor, which is pressed against the stator, is driven by frictional forces due to the elliptic trajectories [1]. The electrical excitation of motor vibrations is applied by a two-phase resonant converter. Due to dielectric properties of the piezoceramic, characterized by a capacitance in each phase, two inductors have to be added in series. Thus, the USM becomes integral part of a series resonant converter feeding the motor with almost sinusoidal voltages.

The prototype version of the ACS is realized without any torque measuring system by open loop torque control. Besides the simple mechanical assembly of the prototype ACS the main advantage of open loop torque control e.g. is the avoidance of a torque sensor and the increase of safety. In chapter 4. a control scheme for open loop torque control is presented which can be modified if a torque measuring system is introduced into the mechanical assembly of the stick. For later application a torque measuring system is used obviously but in the case of failure the control system can be switched and the stick can be operated by open loop torque control, too.
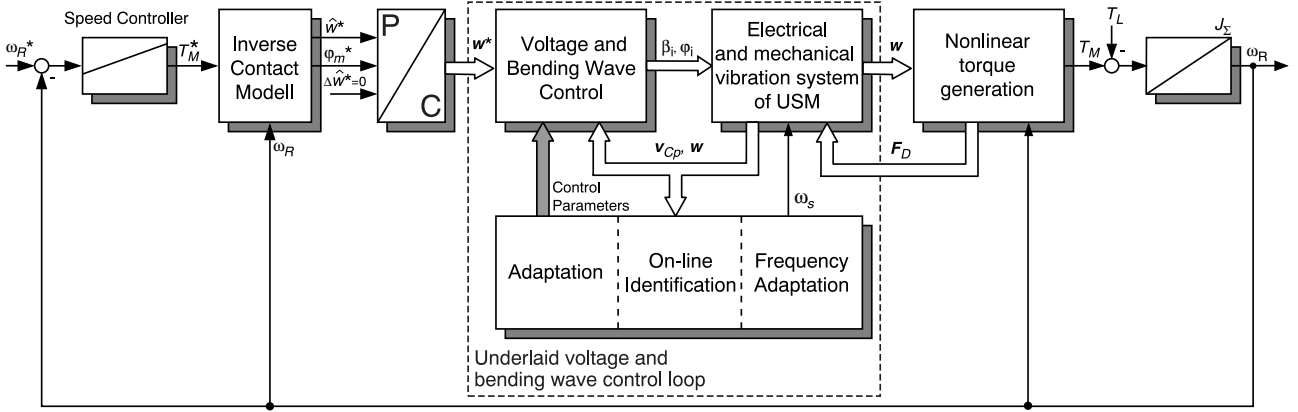
Figure 1. Speed control and open loop torque control by the inverse contact model. The dashed block represents the underlaid voltage and bending wave control loop with on-line identification and adaptation of the controller and switching frequency.

2. BENDING WAVE CONTROL

The speed-torque characteristic is nonlinear related to the bending wave w which in general is represented by a combination of a travelling wave and a standing wave. The result of an open loop torque control will be only satisfying if a bending wave control is stabilizing the mechanical oscillation system eliminating the influences of temperature effects and nonlinearities.

Due to the complex and widely nonlinear characteristics of USMs intensive efforts of research are required for optimizing and exploiting the power performance. The control scheme which is used for the ACS is based on a high performance bending wave control presented in [6]. It controls the time depending fundamental Fourier coefficients of the mechanical oscillations described in their cartesian coordination. Since there are two mechanical vibration systems (orthogonal wave modes) the bending wave is described by four quantities which are united within the vector w (see dashed block in Fig. 1). The bending wave control is based on an averaged model [5] of the motor describing the beat characteristic of the resonant tanks and it is realized by an underlaid voltage control. The control signals are the block width β_i $(i = 1, 2)$ and phase shifts φ_i of the converter stage. Since the eigenfrequency and the damping of the mechanical resonant tanks vary in a wide range due to feedback forces F_D and temperature effects, the controllers and the switching frequency ω_S are adapted by on-line identification of the mechanical oscillation system. Maximum efficiency is obtained by this control scheme by operating the drive in the mechanical resonance frequency while the well known pull-out phenomenon of travelling wave USMs is avoided completely by stabilizing instable operation points. Furthermore a high dynamic behaviour is obtained.

It is also thinkable to use a more simple bending wave control scheme but the performance of the underlaid control schemes influences the performance of the ACS-control decisively.

3. INVERSE CONTACT MODEL AND SPEED CONTROL

For realization of open loop torque control as mentioned before the nonlinear torque generation has to be taken into account. It is caused by the effects within the contact mechanism between the stator surface and the rotor's contact layer. Several contact models for this friction interface have been derived by different researchers, e. g. [3], [4]. Assuming first a static relation between the applied bending wave w, the current rotor speed ω_R and the generated motor torque T_M and second a high dynamic behaviour of the bending wave control, almost linear relations can be obtained by use of the inverse speed/torque-characteristic. This approach is called an inverse contact model, Fig. 1. Using this concept on one hand open loop torque control is feasible and on the other hand it is possible to realize a simple speed control by applying a linear speed controller as well known for conventional electrical drives, Fig. 1.

3.1 Inverse contact model

Available contact models describe only the general effects of the torque generation but there are still some quantitative deviations. In [8] a simple two dimensional basis function network (BFN) trained off-line by measured speed/torque-curves is proposed for realizing the inverse contact model. In order to optimize the performance of the overall drive system a setpoint adjustment is proposed in [8] (see Fig. 2) which serves for minimizing losses by the
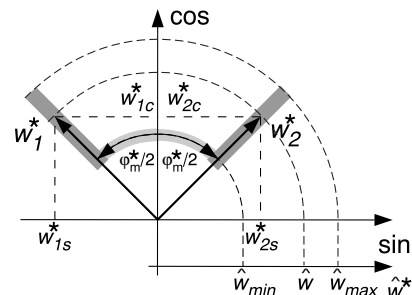

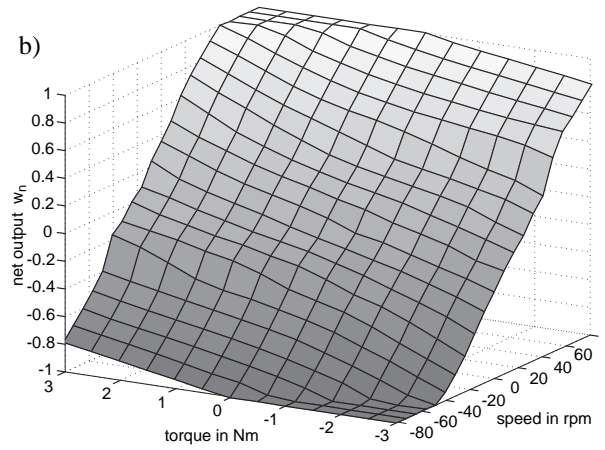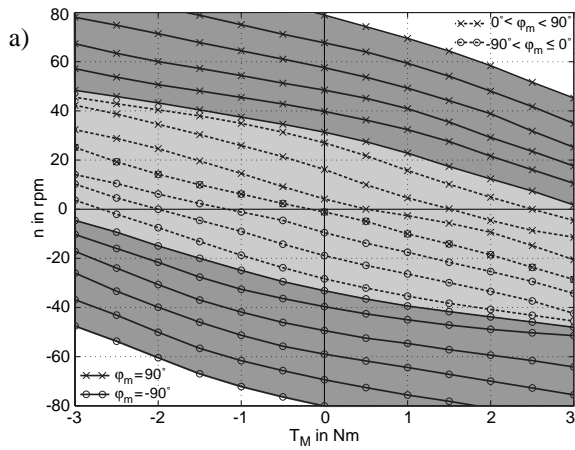**Figure 2.** Setpoint adjustment for optimized operating conditions.

Figure 3. a) Measured speed/torque-curves of the USM.
    b) Two-dimensional BFN for approximation of the inverse contact model.

friction interface also avoiding stick effects at low mechanical amplitudes. The setpoint adjustment is formulated in polar coordinates which are transformed in cartesian coordinates by the transformation block in Fig. 1 ($P \rightarrow C$).

In the upper operation range called high speed/torque-region (marked dark grey in Fig. 2) the operation point is adjusted by varying the bending wave's amplitude $\hat{w}$ keeping a perfect travelling wave (temporal phase shift $\varphi_m = \pm 90$). In the lower operation range called low speed/torque-region (marked light grey in Fig. 2) the bending wave's amplitude $\hat{w}$ is kept to a certain threshold and the operation point is adjusted by varying the temporal phase shift φ_m representing a superposition of a travelling and a standing wave. Fig. 3a shows measured speed torque curves corresponding to the chosen setpoint adjustment. The operation ranges are distinguished by different grey scales (light grey - low speed/torque-region and dark grey - high speed/torque-region). Further a nonlinear transformation is proposed in [8] for describing the setpoint adjustment by only one scalar and normalized value w_n.

Applying this nonlinear transformation a simple two dimensional basis function network (see Fig. 3b) with the desired motor torque T_M^* and the current rotor speed ω_R as input quantities and the normalized value w_n as output quantity are used for realizing the inverse contact model. In [8] the accuracy of the inverse contact model is proven. The deviation of the applied torque are about 15% of the maximum torque value.

3.2 Speed control

Since the nonlinear torque generation of the USM is compensated by the inverse contact model, a linear PI-controller [7] is applied for the speed control as shown in Fig. 1. The amount optimum is used for designing the controller, and a reference filter is applied (which is not shown in Fig. 1). A one mass system is assumed for the rotor's dynamic, and the torque generation is approximated by an appropriate first order lag.

In Fig. 4 measured transient responses of the speed controlled USM are shown. The rotor's speed n, the desired torque T_M^*, the normalized value w_n, the bending wave's amplitude $\hat{w}$ and the phase φ_m are depicted. The left column shows a step command response from the low-speed/low-torque region (operating point P1 with $n = 10$ rpm and $T_L = 0$) into the high-speed/high-torque region (operating point P2 with $n = 50$ rpm and $T_L = 0$). During the first time interval $0 \leq t \leq 3$ ms the reference value of the phase φ_m is increased by the BFN due to reference torque T_M^*, while the reference value of the amplitude is
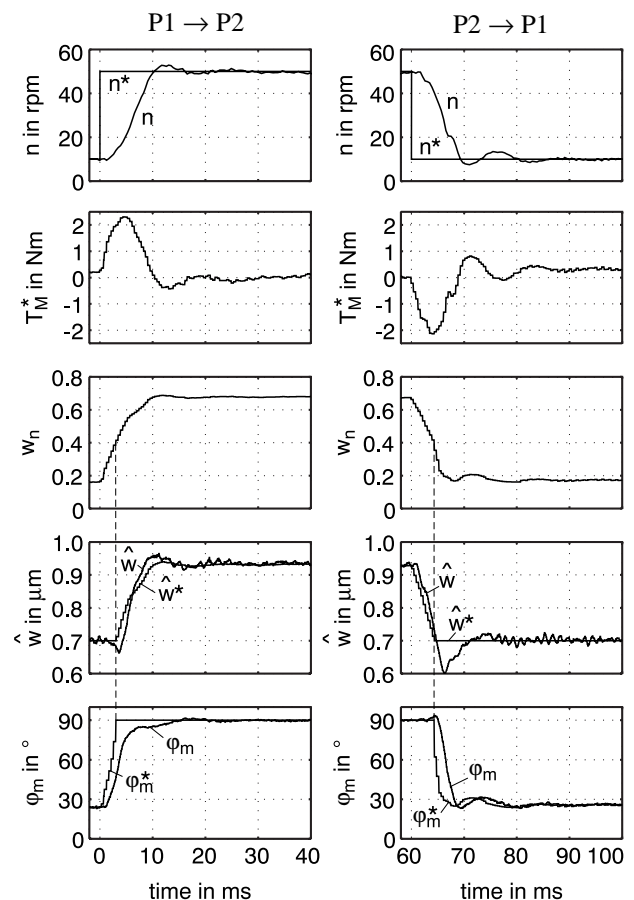

Figure 4. Step command responses of speed controlled USM-drive.

kept to $\hat{w}_{min} = 0{,}7\,\mu m$. When φ_m^* attains its maximum of $90°$ the speed is controlled by varying the reference value of the wave's amplitude $\hat{w}$, whereby the drive is operated with a perfect travelling wave. After a short rise time of about $10\,ms$ the desired speed is attained. Since the USM-drive is accelerated during this response, the corresponding torque-speed trajectory depicted in Fig. 5 passes almost the first (motory) quadrant.

The right column shows the opposite operation mode: $P2 \rightarrow P1$. First, the reference value of the amplitude is decreased to its minimum $\hat{w}_{min} = 0{,}7\,\mu m$, while the phase φ_m^* is kept at $90°$. Second, at $t = 4{,}5\,ms$ and $w_n = 0{,}4$ the speed is regulated finally by the reference value of φ_m. Since the drive is decelerated in this case, the corresponding speed-torque trajectory passes almost the second (non-motory) quadrant as shown in Fig. 5.

Due to the sufficient compensation of nonlinear torque generation by the BFN the response time and overshoot is approximately identical and the system reacts nearly symmetrical in both cases.

Additionally the speed-torque trajectories of a speed reversal ($P3 \rightarrow P2$) and a step-like load change ($P4 \rightarrow P5$) are depicted in Fig. 5. The speed reversal is performed from $n^* = -50\,rpm$ to $n^* = 50\,rpm$ and the reference torque reaches its upper boundary. The step-like load change is performed from zero to $T_L=1\,Nm$.

As indicated by the measurements, first the designed speed control ensures the optimized conditions as outlined by the setpoint adjustment for high-speed/high-torque and low-speed/low-torque operation modes. Second the operation of the BFN, applied for compensation of nonlinearity, operates satisfactorily as indicated by the expected transient responses of a linear speed controller.
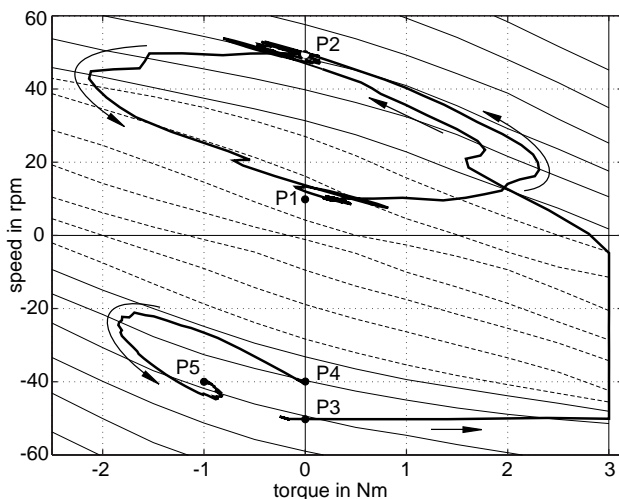

Figure 5. Speed-torque trajectories of speed controlled USM-drive.

4. ACTIVE CONTROL STICK

In order to have simple mechanical assembly an ACS with only one axis is realized which is sufficient for investigations of the control scheme. Additionally a rudder simula-

tor by a DC-motor is realized so that active force feedback can be demonstrated. This prototype ACS has been exhibited and demonstrated several times, for example on a fair March 1999 in the Heinz Nixdorf Museums Forum in Paderborn, see Fig. 6.

4.1 Control scheme

The main function of the ACS is to reproduce the nonlinear spring characteristic which otherwise is generated by the passive mechanic of the stick. An example for a typical characteristic is given in Fig. 10. Different control schemes for the ACS have been investigated.

Since no torque measurement system is available for the prototype ACS the inverse contact model must be used for open loop torque control. First the control scheme shown in Fig. 7 has been realized and tested where the desired torque is calculated from the current stick position by the chosen nonlinear spring characteristic and used directly as input signal of the inverse contact model. Since an instable spring mass system is obtained and a damping measure has to be introduced in the control scheme which is realized by the block square root of local stiffness and the coefficient δ. The torque which is applied by the pilot is described by the disturbance torque T_L.

Figure 6. One axis prototype ACS driven by an USM exhibited and demonstrated on a fair in March 1999 in Paderborn, Germany. Since a DC-motor serves for simulating the rudder actuator active force feedback can be shown by this experimental assembly, too.
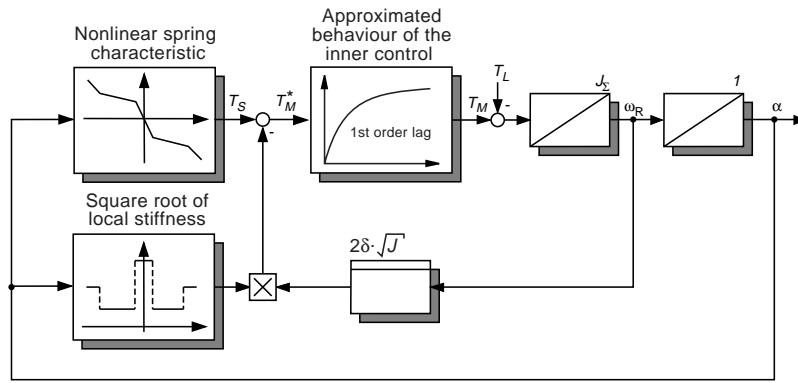
Figure 7. Simple ACS-Control Scheme without underlaid speed control.

This control scheme has some significant disadvantages. For example it is not possible to limit the stick's speed and to integrate a torque measurement system in the control scheme.

Fig. 8a shows simulation results. It is difficult to find an appropriate adjustment for the coefficient δ which guarantees a satisfactory behaviour of the system. Huge deflections of the applied torque can be observed. The piecewise linear spring characteristic and calculation of the damping coefficient affects heavy reactions when the operation range within the spring characteristic is changed. Moreover the stick's speed becomes very high during the simulation.

Thus a further control scheme has been investigated. Since the control scheme has the principal structure of a position control, an ACS control scheme with an underlaid speed and position control has been proven and turned out as an appropriate solution, Fig. 9.

The applied speed control presented in [7] and section 3.2 is overlaid by a simple position control loop realized by a proportional position controller. Since the input quantity of the position controller is the reference position α^*, the inverse relation has to be used for reproducing the spring characteristic.

This new control scheme for the ACS has three main advantages. First its operation is stable without an additional damping measure even if the stick is released. Sec-
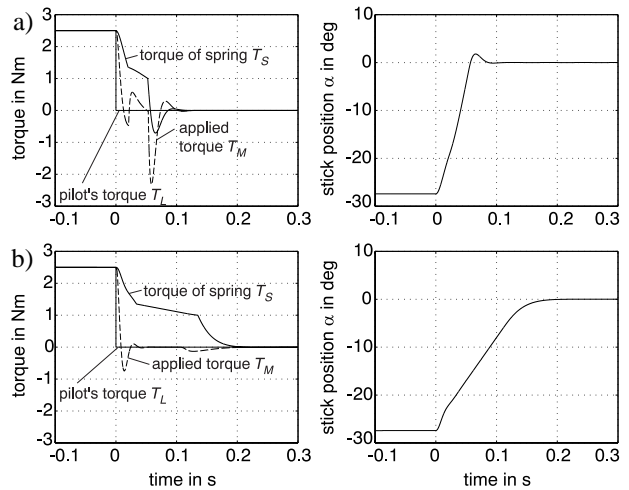

Figure 8. Simulation results of the proposed control schemes.
a) Direct torque controlled system
b) System with underlaid speed and position control.

ond a limitation of the stick's velocity can be realized by just limiting the reference value of the speed controller. Third, the control scheme can be used for operation with torque measuring system (dashed signal lines) and without torque measuring system as shown in Fig. 9. In the first case the measured torque is fed back as input signal for the inverse spring characteristic and in the second case the desired torque of the speed controller is used. For later application a torque measuring system will be used obviously but in the case of failure the control can be switched
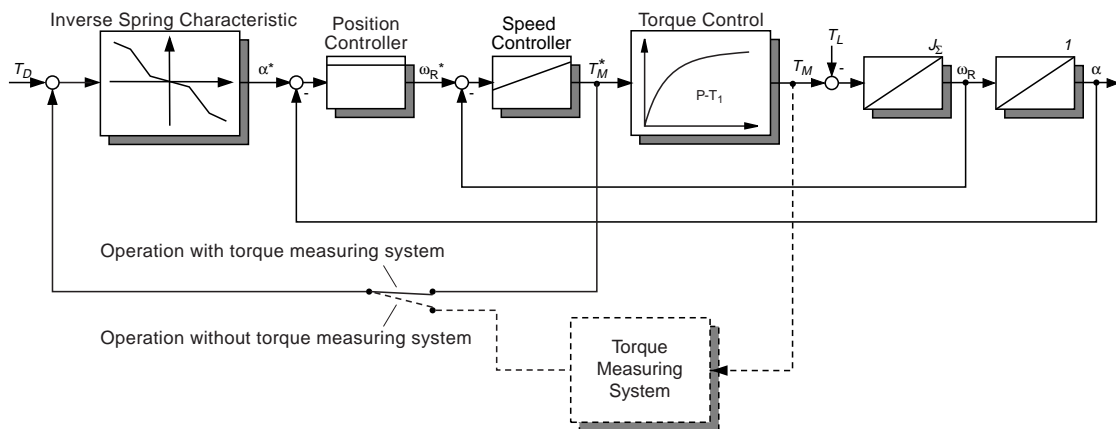

Figure 9. Advanced ACS control scheme including an underlaid speed and position control.

and the stick can be operated by open loop torque control, too. Active force feedback and stick vibrations as a warning signal can be realized by superimposing a torque signal T_D.

As shown in Fig. 8b by the simulation results the reaction of the system is improved significantly. The applied torque now follows the command of the speed controller thus the reaction is almost independent from the nonlinearity of the spring characteristic. The reaction of the system is much slower than in the first case. This is effected by the limitation of the stick's speed to $n_{max} = 60\text{rpm}$.

4.2 Experimental Results

In the case of open loop torque control which is only realized for the prototype ACS the accuracy of the torque generation is depending on the accuracy of the inverse contact model. Fig. 10 shows measured torque curves T_M versus stick position of the realized ACS in comparison with the desired torque T_S^* given by the spring characteristic. The operation range of interest is passed through by constant speed in both directions (**inc**rease of stick position and **dec**rease of stick position) where a position controlled DC-motor serves for applying the load torque. The deviations are about 15% of the maximum value which corresponds to the accuracy of the inverse contact model as expected. They are caused by the approximation of the neural network and temperature effects but cannot be sensed by the pilot. A significant increase of the accuracy can only be reached when torque measurement system is used, see Fig. 9.
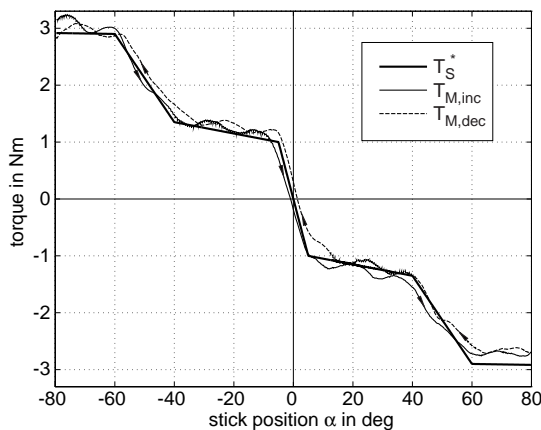
Figure 10. Nonlinear spring characteristic.

5. CONCLUSION

Two control schemes for an ACS driven by a travelling wave type USM and using open loop torque control by a neural network are presented and proven by simulations. The accuracy of the open loop torque control is proven by measurements.

Since this is a first experimental setup of an ACS driven by an USM the results are very satisfactory and significant improvements can only be obtained by use of a torque measurement system.

6. ACKNOWLEDGEMENT

7. REFERENCES

[1] T. Sashida, T. Kenjo: *An introduction to ultrasonic motors.* Clarendon Press - Oxford (1993).

[2] J. Wallaschek: "Piezoelectric ultrasonic motors", *Journal of Intelligent Material Systems and Structures*, Vol.6, January 1995, pp. 71-83.

[3] X. Cao, J. Wallaschek: "Estimation of tangential stress in the stator/rotor-contact of travelling wave ultrasonic motors using visco-elastic foundation models", *2nd Int. Conf. Contact Mechanics 1995*, Ferrara, Italy, July 1995.

[4] J. Maas, P. Ide, N. Fröhleke, H. Grotstollen, "Simulation Model for Ultrasonic Motors powered by Resonant Converters", *IEEE Industrial Application Society Conference 1995 (IAS'95)*, Orlando (Florida), Oct. 1995, pp. 111-120.

[5] J. Maas, H. Grotstollen, "Averaging Model for Inverter-Fed Ultrasonic Motors", *IEEE Power Electronic Specialists Conference 1997*, St. Louis, Vol. 1, 1997.

[6] J. Maas, T. Schulte, H. Grotstollen, "Optimized Drive Control for Inverter-Fed Ultrasonic Motors", *IEEE IAS'97*, New Orleans, Vol. 1, Oct. 1997, pp. 690-698.

[7] J. Maas, T. Schulte, H. Grotstollen: "High Performance Speed Control for Inverter-Fed Ultrasonic Motors by a Neural Network", *ACTUATOR'98*, Bremen, June 1998, pp. 260-263.

[8] J. Maas, T. Schulte, H. Grotstollen: "Controlled Ultrasonic Motor for Servo-Drive Applications", *4th European Conf. on Smart Structures and Materials in conjunction with the 2nd International Conf. on Micromechanics, Intelligent Materials and Robotics, (MIMR´98)*, Harrogate (UK)8, July 1998, pp. 701-708.